Ultra-low-loss polymeric waveguide circuits for optical true-time delays in wideband phased-array antennas

Suning Tang, MEMBER SPIE
Bulang Li, MEMBER SPIE
Nianhua Jiang
Radiant Research, Inc.
3006 Longhorn Blvd., Suite 105
Austin, Texas 78758
E-mail: suning@radiantr.com

Dechang An
Zhenhai Fu
Linghui Wu
Ray T. Chen, FELLOW SPIE
University of Texas at Austin
Microelectronics Research Center
Department of Electric Computer Engineering
Austin, Texas 78758
E-mail: raychen@ut.cc.utexas.edu

Abstract. The optical true-time-delay line is a key building block for modern broadband phased-array antennas, which have become one of the most critical technologies for both military and civilian wireless communications. We present our research results in developing an optical polymer-based waveguide true-time-delay module for multilink phased-array antennas by incorporating wavelength-division multiplexing (WDM) technology. The demonstrated optical polymeric waveguide circuits can provide a large number of optical true-time delays with a dynamic range of 50 ns and a time resolution of 0.1 ps. Various fabrication techniques are investigated for producing ultralong low-loss (0.02 dB/cm) polymeric channel waveguides with tilted waveguide grating output couplers. Fast photodiode arrays are fabricated and rf signals with frequencies of 10 to 50 GHz are generated through the optical heterodyne technique. A detailed study of waveguide amplification to achieve loss-less polymeric waveguide is conducted. The optical amplification of 3.8 dB/cm is achieved at a wavelength of 1064 nm in a Nd^{3+}-doped polymeric waveguide. WDM techniques are also employed for potential multilink applications. The presented methodologies enable hybrid integration with a reduced cost in optoelectronic packaging and an increased reliability and decreased payload for the next generation of phased-array antennas.
 [S0091-3286(00)00603-6]

Subject terms: optical true-time delay; phased-array antenna; polymeric waveguides; waveguide grating; waveguide amplifier; optical waveguide circuit.

Paper IO-06 received June 30, 1999; revised manuscript received Sep. 8, 1999; accepted for publication Sep. 12, 1999.

1 Introduction

The increasing demand on bandwidth and the reliability of airborne communications networks have stimulated the replacement of mechanically scanned antennas by phased-array antennas, which enable independent electronic control of each antenna element, thus increasing the flexibility and the speed of beam forming. In phased-array antennas, the phase and amplitude of each radiating element are traditionally controlled through switching the length of electrical delays feeding the antenna elements. However, to provide broadband capability, future generations of phased-array antennas must be built by invoking the recently developed optical true-time-delay (TTD) technology. Optical TTD lines provide phase shifts to each phased-array antenna element through optical delays via the optical fiber or the waveguide that serves as a carrier for rf signals.

The mechanism of phased-array antennas employing electronically driven antenna elements with individually controllable phase shifts can be described as follows. The wavefront direction of the total radiated carrier wave is controlled through a continuously and progressively varied phase shift at each radiating element, achieving a continuous steering of the antenna. For a linear array radiating elements with individual phase control, the far-field pattern along the direction of Φ can be expressed as[1]

$$E(\Phi,t)=\sum_{n=0}^{N} A_n \exp(i\omega_m t)\exp[i(\psi_n+n\mathbf{k}_m\Lambda\sin\Phi)], \tag{1}$$

where A_n is pattern of the individual element, ω_m is the microwave frequency, $\mathbf{k}_m=\omega_m/c$ is the wave vector, ψ_n is the phase shift, Λ is the distance between radiating elements, and Φ is the direction angle of the array beam relative to the array normal. The dependence of the array factor on the relative phase shows that the orientation of the maximum radiation can be controlled by the phase excitation between the array elements. Therefore, by varying the progressive phase excitation, the beam can be oriented in any direction. For continuous scanning, phase shifters are used to continuously vary the progressive phase. For example, to point the beam at an angle Φ_0, ψ_n is set to the following value:

$$\psi_n=-n\mathbf{k}_m\Lambda\sin\Phi_0. \tag{2}$$

Differentiating Eq. (2), we have

$$\Delta\Phi=-\tan\Phi_0\left(\frac{\Delta\omega_m}{\omega_m}\right)\quad(\text{rad}). \tag{3}$$

It is clear that for a fixed set of ψ_n's, if the microwave frequency is changed by an amount $\Delta\omega_m$, the radiated beam will drift by an amount $\Delta\Phi_0$. This effect increases dramatically as Φ_0 increases. This phenomenon is the so-called ''beam squint,'' which leads to an undesirable drop of the antenna gain in the Φ_0 direction.

For wideband operation, it is necessary to implement optical TTD steering technique such that the far-field pattern is independent of the microwave frequency.[2] In the approach of optical TTD, the path difference between two radiators is compensated by lengthening the microwave feed to the radiating element with a shorter path to the microwave phase front. Specifically, the microwave exciting the $(n+1)$'th antenna element is made to propagate through an additional delay line of length $D_n = nL(\Phi_0)$. The length of this delay line is designed to provide a time delay of

$$t_n(\Phi_0) = (n\Lambda \sin\Phi_0)/c \tag{4}$$

for the $(n+1)$'th delay element. For all frequencies ω_m, ψ_n is given by

$$\psi_n = -\omega_m t_n(\Phi_0). \tag{5}$$

With such a delay setup, when the phase term $n\mathbf{k}_m\Lambda \sin\Phi$ in Eq. (1) is changed due to frequency ''hopping,'' the phase term ψ_n will change accordingly to compensate for the change such that the sum of the two remains unchanged. Thus, constructive interference can be obtained in the direction Φ_0 at all frequencies. In other words, the elemental vector summation in the receiving mode or in the transmit mode is independent of frequency, which is crucial for ultrawide and operation for future phased-array antennas (PAAs).

The existing PAA technologies include microstrip reflecting array antennas with mechanical phasing,[3] fiber grating prisms,[4] and thermo-optically switched silica-based waveguides circuits.[5] These attempts have demonstrated the low-weight potential and some good performance characteristic. Mechanical phased microstrip antennas do not require expensive beam-forming transmission-line networks and/or phase-shifting circuits. The beam steering is provided by the mechanical rotation of each antenna elements. In fiber Bragg grating prism technology, high-performance reflection gratings can be easily fabricated in ultra-low-loss optical fibers, but they require very expensive fast wavelength tunable laser diodes. The thermo-optically switched silica-based waveguide circuit offers excellent delay time control in a compact structure where the length of waveguide is defined by photolithography.

There are several severe problems of these existing approaches. Existing approaches fail to provide high-speed beam steering due to the speed limitation of mechanical driving motors, wavelength-tunable laser diodes, and/or 2×2 thermo-optic switches. The existing approaches also require a large number of expensive components such as miniaturized motors, wavelength-tunable laser diodes, and 2×2 thermo-optic switches, which makes the system impractical for commercial applications. The techniques for improving these existing approaches demonstrated so far, in general, add to system complexity, employ very expensive devices, and/or require extremely difficult fabrication processes.

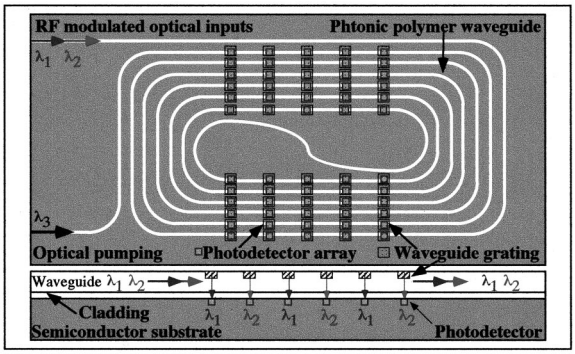

Fig. 1 Schematic diagram of the compact multilink optical TTD line based on a polymer-based photonic waveguide circuit.

2 Polymeric Waveguide Circuits for Optical True-Time Delay

Optical polymers have recently shown great potential for fabricating practical photonic waveguide devices. Because polymeric waveguide technology is conceptionally hybrid, it opens up the possibility for a large-scale optoelectronic integration on any substrate in a cost-effective manner. In this paper, we present a new approach for developing optical TTD lines for wideband PAAs using polymeric waveguide technologies.[6] In this approach, optical TTD lines are composed of photonic polymeric waveguide circuits and electrically switched high-speed photodetectors, as shown in Fig. 1. This PAA system uses an ultralong photonic polymeric channel waveguide circuit on a semiconductor substrate, where a high-speed photodetector array is prefabricated. The photonic polymeric waveguide circuits consist of (1) polymeric channel waveguides, (2) waveguide grating couplers, and (3) waveguide amplifiers. Such a polymeric waveguide circuit is capable of providing optical TTDs from 1 ps to 50 ns for wideband multiple communication links in a compact miniaturized scheme. Note that the bandwidth of this approach is currently limited by the bandwidth of photodetectors at 60 GHz. The optical amplification along the waveguide is important to compensate the optical loss due to the waveguide propagation and grating fanout. The optical heterodyne technique is used for generating an optical rf carrier by employing two coherent laser diodes with slightly different wavelength. A large number of TTD combinations can be provided for the PAA simultaneously by electronic switching the photodetector array fabricated under the polymeric waveguide circuits. This system eliminates the need for fast wavelength tunable laser diodes, long bulky bundles of fibers, and/or expensive optical 2×2 waveguide switches. Unlike any conventional approach where one TTD line can provide only one delay signal at a time, this TTD module is capable of generating all required optical TTD signals simultaneously to all antenna elements.

Compared to expensive electro-optic switches and wavelength-tunable laser diodes, high-performance photodetectors are inexpensive and can be cost-effectively fabri-

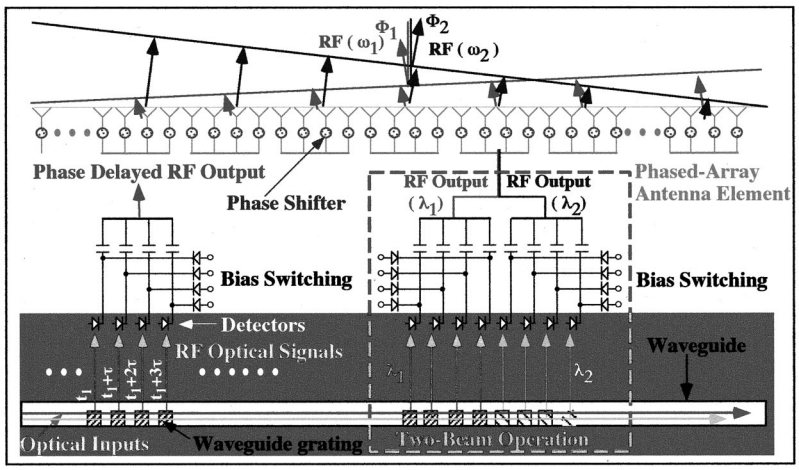

Fig. 2 Electrical diagram of a detector-switched optical waveguide TD line for photonic phased-array antennas.

cated into a large array based on the technologies originally developed for optical imaging and fiber-optic communications. High-speed Newport MSM photodetectors have a bandwidth up to 60 GHz or a rise time of 7 ps. The electrical diagram of the detector-switched optical TTD module is shown in Fig. 2. Such a hybrid integration of detectors to the optical waveguides eliminates the most difficult optoelectronic-packaging problem associated with the delicate fiber-detector interface and/or fiber-switch interface. It not only reduces the cost associated with optoelectronic packaging, but also reduces the system payload with an improved reliability for airborne applications. The TTDs for multiple communication links can be simply provided by employing multiple optical rf modulated beams at different wavelengths over the same delay line based on wavelength-division multiplexing technique.

The unique optical amplification feature of photonic polymers enables us to fabricate an ultralong optical channel waveguide with a large number of fanout gratings.[7] The optical propagation loss and fanout loss are compensated by the optical gain throughout the waveguide delay line. As a result, a large number of time delays can be obtained by using a single laser diode for advanced photonic radar systems that often have 10^3 to 10^5 antenna elements. The optical gain is provided within the photonic polymeric waveguide doped with rare-earth ions such as Nd^{3+} and pumped by a third laser (λ_3) from another end of the waveguide circuit. To obtain uniform fanout, the optical gain in the waveguide section between two fanout gratings can be engineered to exactly compensate the sum of the waveguide propagation loss and optical fanout loss. The delay at each detector is equal to the time of flight along the waveguide circuit to the selected waveguide grating coupler. Because the length of waveguides is defined by photolithography, the optical polymeric waveguide delay lines can provide a 0.1-ps TTD resolution over a 50-ns dynamic range. The thin-film nature of polymers enables us to fabricate the TTD module (made of waveguide circuits and waveguide gratings) on any substrate of interest, using standard very large scale integration (VLSI) technologies originally developed for microelectronics industries.

3 Ultralong Polymeric Channel Waveguide

A high-performance PAA with dynamic range of 50 ns requires the optical polymeric waveguide to be over 10 m to provide sufficient optical TTD. To fabricate such ultralong polymeric waveguide circuits, we have developed three waveguide fabrication technologies:[8–10] (1) the compression-molding technique, (2) the VLSI lithography technique, and the (3) laser-writing technique. Our experimental results indicate that high-performance polymeric waveguide circuits with a waveguide propagation loss less than 0.02 dB/cm can be produced by using these three polymeric waveguide technologies. The compression-molding technique has demonstrated its uniqueness in producing three-dimensional (3-D) tapered waveguide circuits, which are crucial for obtaining efficient optical coupling between the input laser diode and the waveguide circuit. Mass-producible waveguides with excellent repeatability have been obtained by using the VLSI lithography technique, originally developed for fabricating very large scale integrated circuits on silicon wafer. The laser writing waveguide technology has shown its flexibility in fabricating high-performance large-scale polymeric waveguide circuits.

Due to the excellent repeatable results, standard VLSI lithography techniques was selected for fabrication of the 10-m-long polymeric waveguide circuits. Since the length of waveguides is defined by photolithography, the waveguide length can be precisely controlled and circled for more than 10 m with accuracy in the submicrometer range. As a result, the polymeric waveguide delay circuits can be fabricated with a 0.1-ps TTD resolution over a 50-ns dynamic range. We successfully fabricated a 10-m-long polymeric waveguide circuit using the VLSI lithography techniques. Figure 3 shows the 10-m-long polymeric channel waveguide circuit with a waveguide dimension of $5 \times 5\ \mu$m. The waveguide propagation loss is about 0.02 dB/cm measured at $\lambda = 1064$ nm. Ultra-low-loss optical polyimides were employed for the waveguide fabrication. These polyimides have shown excellent optical transmission characteristics with good thermal and chemical stabil-

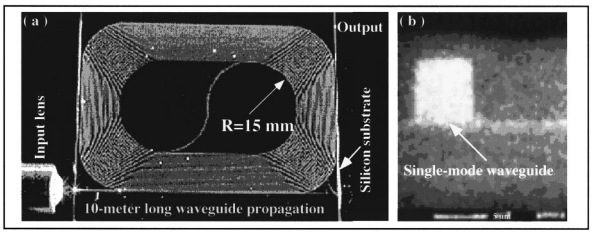

Fig. 3 Photographs of (a) the 10-m-long polymeric waveguide circuit and (b) the waveguide cross section.

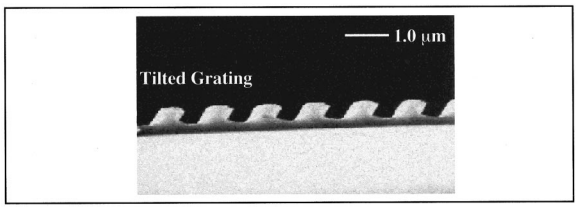

Fig. 4 Scanning electron microscope picture of tilted waveguide gratings.

ity over time and temperature. They have been proven to be silicon complementary metal-oxide semiconductor (CMOS) process compatible.

For a PAA with element-to-element spacing of $d=\lambda/2$, where λ is the wavelength of the rf radiation, the maximum possible delay time is[11]

$$T_{i\,\max}=i\lambda\,\sin\phi_m/2c \quad i=1,2,3,\ldots,K, \tag{6}$$

where θ_m is the maximum scan angle, c is the speed of light, and K is the number of elements of a PAA. The minimum delay corresponding to the antenna angular resolution θ_R is

$$T_{i\,\min}=i\lambda\,\sin\theta_R/2c. \tag{7}$$

Equations (6) and (7) determine the $T_{i\,\max}$ and $T_{i\,\min}$ and the total number R of different delays required for steering the antenna over θ_m with resolution θ_R.

For example, for the designed antenna operating at $f=11\,\text{GHz}$ (or $\lambda=27.3\,\text{mm}$), with $\theta_m=45\,\text{deg}$, $\theta_R=0.7\,\text{deg}$, a 6-bit delay line ($R=2^6=64$) is required with $T_{\max}=2.06\,\text{ns}$ and $T_{\min}=35.6\,\text{ps}$. These correspond to a maximum delay line of $L_{\max}=T_{i\,\max}c/n=42\,\text{cm}$, and a minimum delay step of $L_{\min}=T_{i\,\min}c/n=7.1\,\text{mm}$, respectively. Here $n=1.5$ is the optical refractive index of polymeric waveguide. The antenna element separation is $d=\lambda/2=13.65\,\text{mm}$. The required dimension of the 2-D PAA is $S=(dR)^2=(13.65\times 64)^2=873.6\times 873.6\,\text{mm}^2$. As many as $64\times 64=4096$ antenna elements may be required. Such a 2-D PAA can electronically scan in two dimensions and can cover at least nine satellites at all times in all locations.

4 Tilted Waveguide Grating Couplers for Optical Fanout

To obtain optical TTD, output couplers must be fabricated along the polymeric waveguide at an interval determined by the minimum delay step sized as already described. The optical waveguide grating coupler is an ideal candidate for coupling out the rf modulated optical waves into photodetectors, which propagate through the polymeric waveguide circuit. The unique nonblocking feature of gratings enables us to have a large number of optical fanouts along the waveguide propagation, where each fanout corresponds to a TTD. Since the proposed photonic polymer-based waveguide delay lines are fabricated in a planarized geometry, while the photodetector array employed receives optical signal perpendicular to the substrate surface, surface-normal optical grating couplers are required. To provide effective surface-normal coupling, the microstructure of grating coupler should be tilted for creating the required Bragg phase-matching condition just for one output direction. Such surface-normal waveguide grating couplers are achieved by using tilted-surface relief microstructure.[9,10]

The tilted waveguide grating coupler is fabricated by using the reactive-ion etching (RIE) technique. In this process, the optical channel waveguide is first fabricated using photolithography. The fabricated channel waveguide has a thickness of 10 μm and a width of 50 μm. For simplicity, a glass substrate is selected where waveguide cladding is not required due to the low refractive index of glass. A thin aluminum metal mask is further required on top of the channel waveguide. Then a 500-Å aluminum layer is coated on top of the waveguide using electron-beam evaporation, followed by a layer of 5206E photoresist with spin speed of 3000 rpm. The grating pattern on photoresist was patterned by a photomask, which was then transferred to the aluminum layer by wet etching, to open a grating-like windows on top of the waveguide. We used an RIE process with a low oxygen pressure of 10 mtorr to transfer the grating pattern on the aluminum layer to the polyimide layer. A Faraday cage[12] was used in the RIE process. To form the tilted grating pattern on the polyimide waveguide, the sample is placed at a tilted angle of 40 deg with respect to the incoming oxygen ions inside the cage. The final step was to remove the aluminum mask by another RIE process. The waveguide tilted grating couplers were successfully fabricated. Figure 4 shows the scanning electron microscope picture of the tilted waveguide grating fabricated.

The gratings are designed to surface-normally couple the laser beam out of the waveguide at an operating wavelength of 1060 nm. A large number of gratings can be fabricated on top of the waveguide simultaneously. The output coupling efficiency is measured at 5% when a YAG laser with output wavelength of 1060 nm is employed. Coupling efficiency can be well controlled by adjusting the grating depth from 1 to 8%. The nonblocking nature of the waveguide grating enables a large number of fanouts along the waveguide propagation. In other words, a large number of optical TTDs can be generated along the waveguide propagation with the delay time equal to the time of flight along the waveguide circuit.

5 Polymeric Waveguide Amplification for Lossless Operation

Optical waveguide amplification provides a convenient way to amplify optical signals without the need for optoelectronic conversion. Due to the large number of optical fanouts in a very long waveguide delay line, an optical

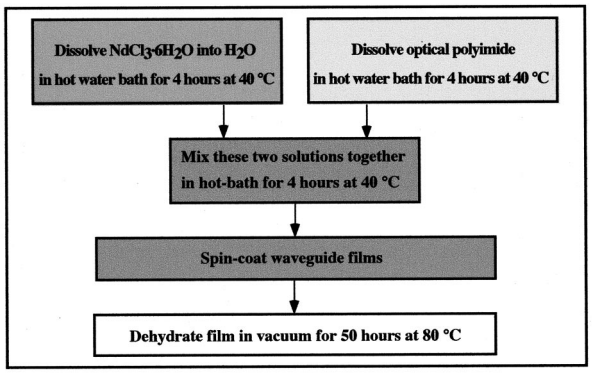

Fig. 5 Fabrication procedures for preparing a lossless photonic polymeric waveguide film.

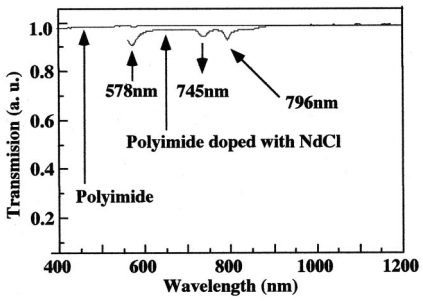

Fig. 6 Transmission spectra of polymeric waveguide films for pure polyimide film and polyimide film doped with 2.1% (by weight) $NdCl_3$.

waveguide amplifier is highly desired for fabricating a detector-switched optical waveguide TTD module. The resulting signal amplification is crucial to compensate the optical fanout loss and propagation loss for creating a ''lossless'' optical waveguide delay line.[8,13–18] Realization of lossless optical waveguides based on photonic polymers represents a new technology that may create a new class of photonic devices with superior performance at a reduced cost. The application of the lossless photonic polymer to the optical TTD module would eliminate the necessity using multiple input laser diodes that must be operated coherently not only in frequency but also in phase. It also enables uniform optical outputs to each photodetector by adjusting the optical gain of the waveguide equal to the sum of optical propagation loss and fanout loss. Such a lossless photonic polymer is obtained by doping rare-earth ions such as Nd^{3+} in a host polyimide.

To develop a photonic polymeric amplifier, the rare-earth ions must be doped uniformly in the host polymer. Since organic solvents are often used to prepare the polyimide solution, while rare-earth ions such as $NdCl_3$ are highly soluble in water, it is reasonable to use a mixture of water and an organic material as the solvent. Figure 5 shows the developed preparation procedure for photonic polymers. The host polyimide is first dissolved in an organic solvent and kept in hot bath for 4 h at 40°C. The $NdCl_3 \cdot 6H_2O$ is dissolved in pure water solvent, and kept in hot bath for 4 h at 40°C. Then, the two solutions were mixed together and put in hot water bath at 40°C for another 4 h. A uniform solution containing Nd^{3+} ions is thus formed. The quality of the solution is pivotal to make high-performance optical waveguide amplifiers. Polymeric thin films are obtained by spin-coating the polymer on silicon substrate, and dried in vacuum at 80°C. The thickness of the film can be well controlled within 1 to 10 μm by adjusting the spin speed and/or polymer concentration.

To optimize the optical amplification efficiency, the fluorescence lifetime of the metastable states of doped Nd^{3+} ions must be kept long. It is well known that the most serious quenchers are the admixed O–H groups from water molecules for glass waveguides.[19,20] The underlying mechanism is due to the vibronic coupling between the effective phonons and the metastable electronic states of Nd^{3+} though overtone vibration. If the energy gap between the excited state and the ground state of Nd^{3+} is less than four times of the phonon frequency, the fluorescence of the metastable state will be fully quenched.[20,21] Therefore we developed an effective dehydration process to eliminate the water molecules within the polymer.[8,13,14] The transmission spectra of two samples, a pure polyimide film and a Nd^{3+}-doped polyimide film, are shown in Fig. 6, measured by a Lambda spectrometer. Within the range of 500 to 1200 nm, three main absorption bands of Nd^{3+} were observed, centered at 578, 745, and 796 nm. The absorption spectrum due to Nd^{3+} is very similar to that of Nd^{3+}-doped silica fibers.[21]

We experimentally demonstrated the optical amplification in the photonic polymeric waveguides fabricated. Figure 7 shows the setup for optical gain measurement. The waveguide under test was mounted on a prism coupling stage. The pumping beam at wavelength of 796 nm, from a tunable Ti:sapphire laser, was coupled into the waveguide using prism P_1. The 1064-nm signal beam was provided by a Nd:YAG laser and coupled into the waveguide using prism P_2. Note that P_1 also functions as the output prism for the signal beam. The pumping beam and the signal beam were carefully aligned to ensure the overlap with each other to achieve the optimum amplification. A laser beam analyzer and an IR CCD camera were employed for the alignment. The 1064-nm amplified signal was detected after passing through a wavelength-filtering system containing rejection filter F_1 and a laser bandpass filter F_2, both working at 1064 nm.

The relationship among the optical gain, pumping power, Nd^{3+} doping concentration, and the interaction length of the signal and pump beams was experimentally investigated. Figure 8 shows the variation of optical gain versus the pumping power with a Nd^{3+} doping concentration of $6.7 \times 10^{19}/cm^3$. The interaction length of the signal and pumping beams in the waveguide was fixed to 1.8 cm. A saturated gain of 3.8 dB was observed, corresponding to a pump power of 4.9 mW. The relationship between the gain and the concentration of Nd^{3+} is further illustrated in Fig. 9. The optimized concentration of Nd^{3+} for amplification was $\sim 6.7 \times 10^{19}/cm^3$. Gain quenching occurred seriously when the Nd^{3+} doping concentration was determined at $\sim 7.8 \times 10^{19}/cm^3$.

Nd^{3+} has two broad absorption bands centered at 745 and 796 nm, as indicated in Fig. 6. These absorption bands

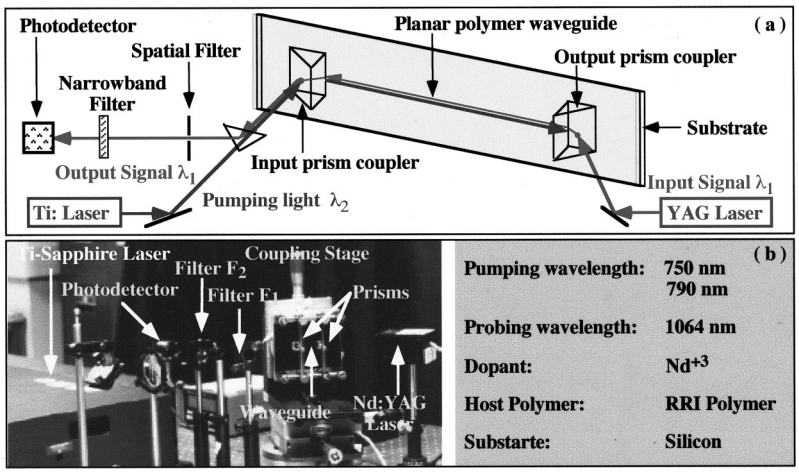

Fig. 7 (a) Schematic of the test setup for demonstrating optical amplification in polymeric waveguides and (b) photograph of the experiment setup and test parameters.

were further confirmed by the measuring the gain versus pumping wavelength, as shown in Fig. 10. The pumping efficiency reached maximum around 745 and 796 nm and decreased slowly when the pump wavelength was detuned away from the peaks. This result confirms that the energy levels of Nd^{3+} in amorphous polymer are similar to these in amorphous glasses. In short, the rare-earth ions of Nd^{3+} were successfully doped into the host polymer. Optical amplification of a photonic polymeric waveguide were demonstrated with 3.8 dB net gain at $\lambda = 1064$ nm in a 1.8-cm-long planar waveguide.

6 Generation of Wideband rf Signals Using the Optical Heterodyne Technique

To provide the ultrawideband operation from 11 to 40 GHz, several rf techniques can be employed with different bandwidth-tunable capabilities. These include harmonic generation in a Mach-Zehnder modulator,[22] heterodyne mixing of two lasers,[23] resonance enhanced modulation of a laser diode[24] (LD), and a dual-mode distributed feedback (DFB) laser in mode-locked operation.[25] Direct modulation of the LD seems straightforward to generate a millimeter wave. However, the high insertion loss, high drive voltage, nonlinear response, and small modulation depth limit the usefulness of this technique.[26]

Compared with direct modulation of an LD or using external modulators, the optical heterodyne technique is capable of providing hundreds of gigahertz base bandwidths while maintaining a high modulation depth. We have successfully generated up to 50-GHz rf signals using two tunable LDs oscillating at single longitudinal mode based on optical heterodyne technique. Figure 11 shows the schematic diagram of the experimental setup. The outputs from these two lasers with slightly different wavelengths are combined by a two-to-one polarization maintaining fiber beam combiner and then sent to wideband photodetector.

Suppose that the outputs of these two lasers are given by

$$E_1(t) = A_1 \exp(j\omega_1 t), \tag{8}$$

$$E_2(t) = A_2 \exp(j\omega_2 t) = A_2 \exp[j(\omega_1 + \Delta\omega)t], \tag{9}$$

where $\Delta\omega$ is the beat frequency. The output of the photodetector is given by[23]

$$i_d(t) = \frac{e\eta}{h\nu}[A_1^2 + A_2^2 + 2F(\Delta\omega)A_1A_2\cos(\Delta\omega)t], \tag{10}$$

where e is the electron charge, η is the quantum efficiency of the detector, $h\nu$ is the photon energy, and $F(\Delta\omega)$ is the frequency response function of photodetector.

Due to the limitation of the bandwidths of microwave amplifier and the spectrum analyzer, this 50-GHz signal cannot be detected directly. To solve this problem, a third

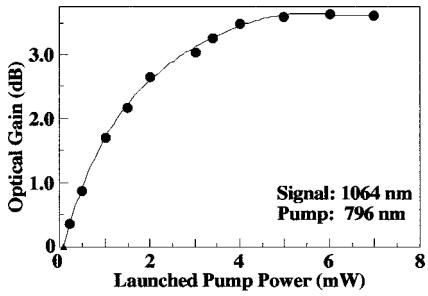

Fig. 8 Measured optical gain in Nd^{3+}-doped polymeric film at $\lambda = 1064$ nm as a function of optical pumping power at $\lambda = 796$ nm.

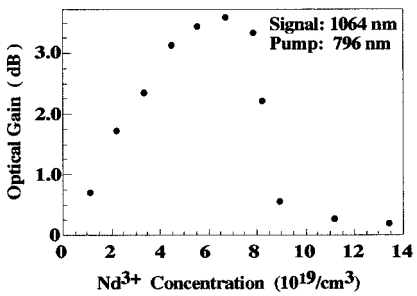

Fig. 9 Measured optical gain at $\lambda = 1064$ nm as a function of Nd^{3+} concentration in an optical polyimide waveguide.

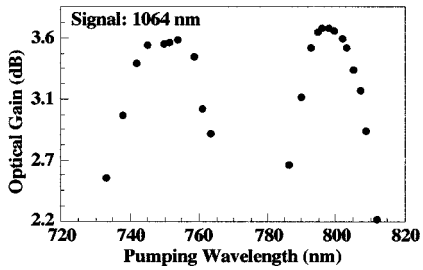

Fig. 10 Variation of optical gain at 1064 nm versus pumping wavelength. The optical pumping power is fixed at 5 mW in the measurement.

tunable diode laser with wavelength between the preceding two lasers is used to down-convert this 50-GHz signal to two signals at about 25 GHz. This 50-GHz signal was sent directly through the optical waveguide delay line fabricated. The optical fanout from the waveguide TTD line is combined with the output of the third laser and is then sent to an ultrafast photodetector with a 25-GHz microwave amplifier, which is connected to an rf spectrum analyzer. The measured signals of $\Delta\omega=\omega_1-\omega_2=(\omega_1-\omega_3)+(\omega_3-\omega_2)$ $=24.85+25.90=50.75$ GHz is shown in Fig. 12.

7 Detector-Switched Optical True-Time-Delay Lines

Figure 13 shows a photo of a polymeric waveguide TTD line fabricated on an 8-cm-long glass substrate with waveguide thickness of 10 μm and width of 50 μm. Surface-normal waveguide grating couplers are fabricated with a 50-μm coupling length and a 10-mm separation. The optical rf signals, propagating through the channel waveguide, are coupled surface-normally into a high-speed two-photodetector array, placed right under the waveguide delay line. The electrical output of two high-speed photodetectors are electrically combined with a single output. The bandwidth of these detectors is ~60 GHz with a 5-V bias voltage. The output of the electrical response from the detectors is first amplified through a 20-GHz microwave amplifier and then connected to a sampling scope for measuring the optical true delay times. The schematic diagram for measuring the optical TTDs is also illustrated in Fig. 13. In the experiment, the delay time interval of the optical waveguide TTD line is measured by employing a Ti:sapphire

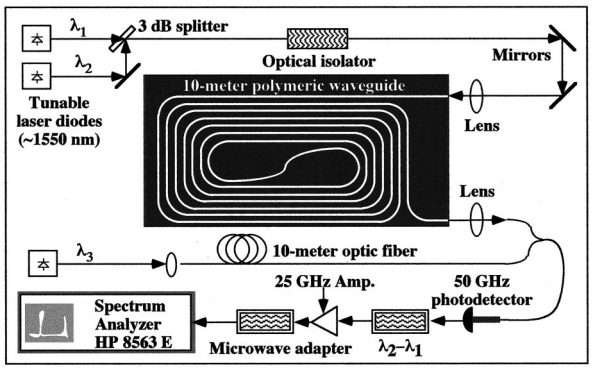

Fig. 11 Generation of rf signals using the optical heterodyne technique.

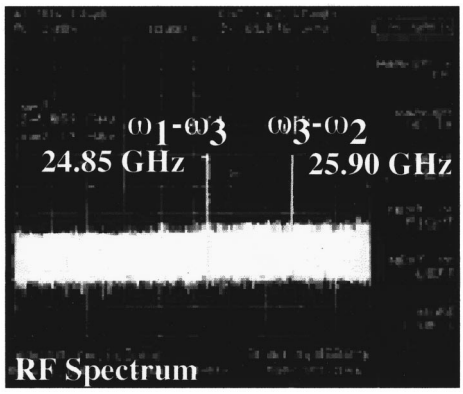

Fig. 12 Indication of a 50.75-GHz optical rf signal generated by optical heterodyne technique.

femtosecond laser system. Sequential equivalent time sampling technique is employed for measuring the small time delay (~50 ps). Since the delay signal is repetitive, samples can be acquired over many repetitions of the signal, with one sample taken on each repetition. When a synchronous trigger is detected, a sample is taken after a very short, but well-defined delay. When the next trigger occurs, a small time increment is added to this delay and the scope takes another sample. This process is repeated many times until the time window is filled. This enables the oscilloscope to accurately capture signals whose frequency components are much higher than the scope's sample rate. A 50-ps delay interval, corresponding to a 10-mm fanout separation of the polymeric waveguide delay line, is obtained using this setup and the result is also illustrated in Fig. 13. The uncertainty due to jittering is estimated to be less than 5 ps for this experiment.

The detector bias switching is successfully obtained by lunching a short electrical pulse into the photodetector bias circuit while monitoring the photodetector output response under cw optical rf illumination. Figure 14 shows the electrical diagram of the experiment. A 500-ps electrical pulse is coupled into the detector bias circuit. A high-speed electro-optic response is obtained at the photodetector output end. The output pulse is measured with a linewidth of 1 ns, which implies a nanosecond switching speed for the photodetector-switched optical polymeric waveguide TTD line.

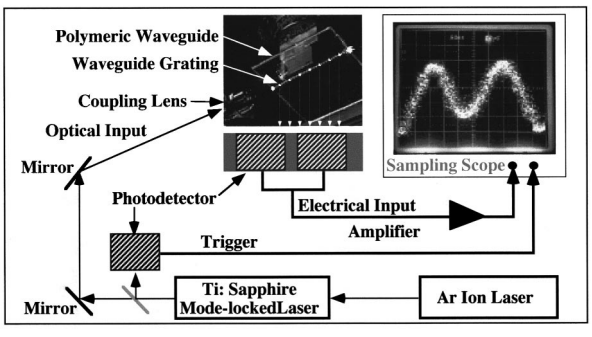

Fig. 13 Schematic diagram for measuring the optical TTDs using a femtosecond Ti:sapphire laser system.

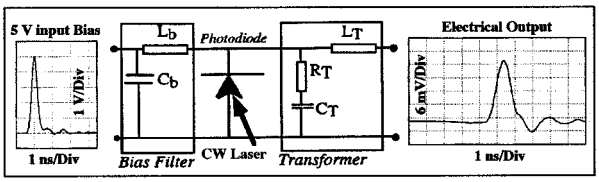

Fig. 14 Electric diagram for measuring the switching speed of biased photodetectors.

8 Wavelength-Division Multiplexing in Polymeric Channel Waveguides

To provide the multilink optical TTD functionality, the wavelength-division multiplexing (WDM) technique can be employed in conjunction with polymeric waveguide grating couplers. Waveguide grating couplers are ideal for producing a large number of optical rf modulated TTD signals to photodetectors when the WDM technique is employed for multilink communications. The unique nonblocking feature enables us to have a large number of optical fanouts from multiple laser beams along the waveguide propagation. Because of the strong wavelength selectivity of optical gratings, waveguide gratings can be designed and fabricated to diffract light at a desired wavelength by adjusting grating period. In other words, it can function as a wavelength-division demultiplexer in the waveguide delay line circuits when multiple laser beams are used for multiple communication links.

To demonstrate the concept of a simple multilink approach, a set of waveguide surface-normal grating couplers with operating wavelengths of $\lambda_3 = 1550$ nm were fabricated over a polymeric waveguide delay line. In the experiment, three laser beams with output wavelength at $\lambda_1 = 950$ nm, $\lambda_2 = 1300$ nm, and $\lambda_3 = 1550$ nm, respectively, were employed and coupled into the testing waveguide delay line, as shown in Fig. 15. To determine the optical crosstalk among the multiple channels, three input lasers were further amplitude modulated at three different frequencies (0.9, 0.7, and 1.1 MHz), respectively. This enabled us to separate the measured crosstalk and signal on the display screen simultaneously. The input power of each modulated laser beam was adjusted at the same level ($\sim$500 μW). The optical output from a grating coupler was detected by a fiber pig-tailed photodetector through a fiber graded-index (GRIN) lens. In the experiment, the detector was positioned at the waveguide grating coupler designed for surface-normal coupling at $\lambda = 1550$ nm. The fabricated waveguide grating has a 30-μm interaction length with a coupling efficiency of 5%. The optical crosstalk was measured by an rf spectrum analyzer (Model hp 8566B). The channel crosstalk was successfully determined at a signal-to-noise ratio (SNR) of 32 dB, as shown in Fig. 16. A tunable laser with a wavelength tuning range from 1470 to 1650 nm was further used to determine the coupling window of waveguide gratings. The measured transmission spectrum had a 40-nm, 3-dB linewidth with a 100-nm wavelength separation between the first two minima.

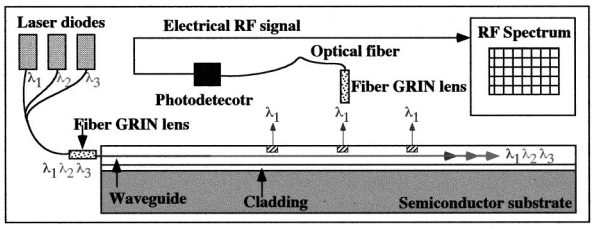

Fig. 15 Schematic of a multilink waveguide delay line using the WDM technique.

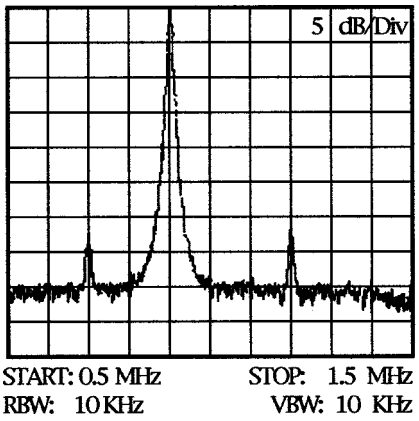

Fig. 16 Measured optical signal at $\lambda_1 = 1550$ nm and optical crosstalk from two other channels at $\lambda_1 = 950$ nm and $\lambda_1 = 1300$ nm, respectively.

9 Conclusions

We successfully demonstrated a photonic waveguide-based TTD line using polymeric waveguides, waveguide amplifiers, and wavelength-selective grating couplers in conjunction with bias-switched photodetectors. Polymeric waveguide technology, including ultra-low-loss polymeric waveguides, optical waveguide amplifiers, and wavelength-selective grating couplers in conjunction with bias-switched photodetectors, offers a unique hybrid integration in realizing advanced photonic PAAs based on optical TTD lines. Such a hybrid integration of photonic devices eliminates the most difficult optoelectronic packaging problem in developing advanced photonic PAAs. This integrated approach not only reduces the cost associated with optoelectronic packaging, but also reduces the system payload with an improved reliability for airborne applications. Currently, all of the building blocks essential for the fabrication of wideband PAAs are becoming available, while the electrically switched optical polymeric waveguide delay lines certainly present a very promising technology in this field.

Acknowledgments

This research is supported by the Ballistic Missile Defense Organization (BMDO), the Air Force Office of Scientific Research (AFOSR), the Office of Naval Research (ONR), the 3M Foundation, and Raytheon Systems Co.

References

1. E. Brookner, *Practical Phased-Array antenna systems*, Artech House, Boston (1991).
2. J. E. Midwinter, *Photonics in Switching*, Academic Press, Boston (1993).
3. J. Huang, ''Microstrip reflecting antennas with mechanical phasing,'' *NASA Technical Briefs* **20**(12), 54 (Dec. 1996).
4. H. Zmuda, R. A. Soref, P. Payson, S. Johns, and E. N. Toughlian,

''Photonic beamformer for phased array antennas using a fiber grating prism,'' *IEEE Photonics Technol. Lett.* **9**(2), 241–243 (1997).
5. K. Horikawa, I. Ogawa, T. Kitoh, and H. Ogawa, ''Photonic integrated beam forming and steering network using switched true-time-delay silica-based waveguide circuits,'' *IEICE Trans. Electron.* **E97-C**(1), 74–79 (1996).
6. S. Tang, L. Wu, Z. Fu, D. An, Z. Han, and R. T. Chen, ''Polymer-based optical waveguide circuits for photonic phased array antennas,'' *Proc. SPIE* **3632**, 250–261 (1999).
7. R. T. Chen, M. M. Li, S. Tang, and D. Gerold, ''Nd_3^+-Doped graded index single-mode polymer waveguide amplifier working at 1.06 and 1.32 μm,'' *Proc. SPIE* **2042**, 462–463 (1993).
8. S. Tang, L. Wu, F. Li, T. Li, and R. Chen, ''Compression-molded three-dimensional tapered optical polymeric waveguides for optoelectronic packaging,'' *Proc. SPIE* **3005**, 202–211 (1997); and *IEEE Photonics Technol. Lett.* **9**(12), 1601–1603 (1997).
9. S. Tang, T. Li, F. Li, M. Dubinovsky, R. Wickman, and R. T. Chen, ''Board-level optical clock signal distribution based on guided-wave optical interconnects in conjunction with waveguide hologram,'' *Proc. SPIE* **2891**, 111–117 (1996).
10. R. T. Chen, S. Tang, F. Li, M. Dubinovksy, J. Qi, C. Schow, J. Campbell, and R. Wickman, ''Si CMOS process compatible guided wave optical interconnects for optical clock signal distribution,'' in *IEEE MPPOI'97*, Vol. 4, pp. 10–24 (1997).
11. H. Zmuda and E. N. Toughlian, *Photonic Aspects of Modern Radar*, Chaps. 13 and 17, Artec House, Norwood, MA (1994).
12. M. Hagberg, N. Eriksson, and A. Larsson, ''High efficiency surface emitting lasers using blazed grating outcouplers,'' *Appl. Phys. Lett.* **67**(25), 3685–3687 (1995).
13. R. T. Chen, S. Tang, T. Jannson, and J. Jannson, ''45-cm long compress-molded polymer-based optical waveguide bus,'' *Appl. Phys. Lett.* **63**(8), 1032–1034 (1993).
14. S. Tang, R. T. Chen, and M. A. Peskin, ''Packing density and interconnection length of a highly parallel optical interconnect using polymer-based, single-mode waveguide arrays,'' *Opt. Eng.* **33**(5), 1581–1586 (1994).
15. R. Yoshimura, M. Hikita, S. Tomaru, and S. Imamura, ''Very low loss multimode polymeric optical waveguides,'' *Electron. Lett.* **33**(14), 1240–1241 (1997).
16. S. Tang, T. Li, F. Li, M. Dubinovsky, R. Wickman, and R. T. Chen, ''Board-level optical clock signal distribution based on guided-wave optical interconnects in conjunction with waveguide hologram,'' *Proc. SPIE* **2891**, 111–117 (1996).
17. R. T. Chen, M. M. Li, S. Tang, and D. Gerold, ''Nd^{3+}-Doped graded index single-mode polymer waveguide amplifier working at 1.06 and 1.32 mm,'' *Proc. SPIE* **2042**, 462–463 (1993).
18. T. C. Lubensky and P. A. Pincus, *Phys. Today*, p. 44 (Oct. 1984).
19. C. B. Layne and M. J. Weber, ''Multiphonon relaxation of rare-earth ions in beryllium-fluoride glass,'' *Phys. Rev. B* **16**, 3259–3261 (1977).
20. V. P. Gapontsev, S. M. Matitsin, A. A. Isineer, and V. B. Kravchenko, ''Erbium glass lasers and their applications,'' *Opt. Laser Technol.* **14**(4), 189–196 (1982).
21. J. R. Armitage, ''Three-level fiber laser amplifier: a theoretical model,'' *Appl. Opt.* **27**, 4831–4836 (1988).
22. J. J. O'Reilly and P. M. Lane, ''Fiber-supported optical generation and delivery of 60 GHz signals,'' *Electron. Lett.* **30**(16), 1329–1330 (1994).
23. G. J. Simonis and K. G. Purchase, ''Optical generation, distribution, and control of microwaves using laser heterodyne,'' *IEEE Trans. Microwave Theory Tech.* **38**(5), 667–669 (1990).
24. J. B. Georges, M.-H. Kiang, K. Hepell, M. Sayed, and K. Y. Lau, ''Optical transmission of narrow-band millimeter-wave signals by resonant modulation of monolithic semiconductor lasers,'' *IEEE Photonics Technol. Lett.* **6**(4), 568–570 (1994).
25. C. R. Lima, D. Wake, and P. A. Davis, ''Compact optical millimeter-wave source using a dual-mode semiconductor laser,'' *Electron. Lett.* **31**(5), 364–366 (1995).
26. K. Kitayama, ''Highly stabilized millimeter-wave generation by using fiber-optic frequency-tunable comb generator,'' *IEEE J. Lightwave Technol.* **15**(5), 883–893 (1997).

Suning Tang is chief scientist with Radiant Research, Inc., Austin, Texas. He received his BS degree in electrical engineering in laser devices from Nanjing Institute of Technology, China, his MS degree in optics from the Weizmann Institute of Science, Israel, and his PhD degree in electrical engineering in optoelectronic interconnects from the University of Texas at Austin. He was with Cirrus Logic and Advanced Photonics Technologies for 4 years before he joined Radiant Research, Inc. His work in the past 15 years has included optical interconnects, polymer-based waveguide devices, holographic devices, fiber optic devices, optical modulators/switches, optical control of microwave signals, and semiconductor photonic devices. He has been the principal investigator for many awarded SBIR research programs sponsored by the Department of Defense and by private industries. Dr. Tang has chaired several international conferences organized by SPIE, he has published more than 50 papers in IEEE, OSA, AIP, and SPIE journals and holds several patents, and he is a member of SPIE and OSA.

Ray T. Chen is the Temple Foundation Endowed Professor at the University of Texas, Austin. His research includes GaAs all-optical 2-D cross bar switch arrays, 2-D and 3-D optical interconnections, polymer-based integrated optics for true-time-delay lines, polymer waveguide amplifiers, graded index polymer waveguide lenses, active optical back planes, traveling wave polymer waveguide switching devices, and holographic optical elements. Dr. Chen has chaired and was a program committee member for more than 10 domestic and international conferences organized by SPIE, IEEE, and PSC. He is also the invited lecturer for the short course on optical interconnects for the international technical meetings organized by SPIE. Dr. Chen has published more than 130 papers and has delivered numerous invited talks for professional societies. He is a fellow of SPIE and a member of IEEE, OSA, and PSC.

Biographies of the other authors not available.